American Journal of Applied Chemistry
2026, Vol. 14, No. 2, pp. 30–41
https://doi.org/10.11648/j.ajac.20261402.12

SciencePG
Science Publishing Group

Research Article

# Chemical Removal of Toxic Heavy Metals in Acid Mine Drainage Using Hydrazine as Reductant

**Alegbe Mondat John[1, 2, *], Moronkola Bridget Adekemi[1], Fatoba Oolanrewaju Ojo[2], Adekolurejo Ezekiel[1, 3], Agboola Olugbenga Ayodeji[1, 4], Oyesomi Aisha[1], Petrik Leslie Felicia[2]**

[1]Department of Chemistry, Lagos State University, Lagos, Nigeria

[2]Enviromental and NanoSciences Group Chemistry Department, University of the Western Cape, Bellville, South Africa

[3]Department of Science Laboratory Technology, Ogun State Institute of Technology, Igbesa, Nigeria

[4]Department of Chemistry Education, Lagos State University of Education, Oto/Ijanikin, Nigeria

## Abstract

Acid mine drainage (AMD) wastewater generated from coal field mining activities going on in Mpumalanga Province in Republic South Africa contained toxic heavy metals which is harmful to human health and the environment, as it is required to be removed before discharged into the natural water body. The aim of this study is to remove toxic heavy metals (Hg, Th, Cr, Mn, Pb, As, Cd and Ba) from AMD using hydrazine ($N_2H_2$) as reductant. Chemical reduction method was used to remove the toxic heavy metals. Physicochemical analysis was carried out on the mine wastewater. Digestion method was also conducted on the acid mine wastewater. Quantification techniques used in this study are inductively coupled plasma optical emission spectroscopy (ICP-OES), ion chromatography (IC), X-ray diffraction (XRD), X-ray Fluorescence (XRF), transmission electron microscopy (TEM), FTIR and scanning electron microscopy energetic dispersion spectroscopy (SEM-EDS). The results of the maximum concentration and percent removal of heavy metals removed in the AMD using 1.0 M of $N_2H_2$ reductant solution are Hg (0.00019 mg/L, 82.49%), Th (3E-06 mg/L, 99.98%), Cr (0.0078 mg/L, 96.53%), Mn (22.31 mg/L, 82.54%), Pb (0.0004 mg/L, 89.04%), As (0.0009 mg/L, 98.32%), Cd (0.0028 mg/L, 99.09%), and Ba (0.0021 mg/L, 92.00%). The results of the maximum contact time of 120 minutes and percent removal of heavy metals removed in the AMD are Hg (0.00012 mg/L, 89.17%), Th (0.0014 mg/L, 92.49%), Cr (0.013 mg/L, 94.34%), Mn (10.53 mg/L, 91.68%), Pb (0.002 mg/L, 94.91%), As (0.005 mg/L, 90.93%), Cd (0.014 mg/L. 95.37%), and Ba (0.002 mg/L, 90.90%). The optimum concentration was 0.6 M $NaBH_4$ reductant solution and contact time was 30 minutes. The concentration removal of the heavy metals in the treated AMD revealed that the maximum concentrations of some metals are within the WHO while the others are above WHO limits. In conclusion, $N_2H_4$ reductant removed most of the toxic heavy metals effectively in the AMD solution with brownish precipitate formed without generating sludge was identified to be $Fe^0$ nanoparticles.

## Keywords

AMD, Physicochemical Analysis, Digestion, Chemical Reduction, ICP-OES Quantification

*Correspondence: Alegbe Mondat John (alegbemj@gmail.com)

**Received:** 10 April 2026; **Accepted:** 28 April 2026; **Published:** 11 May 2026

# 1. Introduction

Acid mine drainage (AMD) is an environmental problem that is generated from the mining activities of excavating mineral resources from the earth, when mineral sulphides especially iron sulphides, marcasite ($FeS_2$), magnetite ($Fe_3O_4$), and pyrite are predominant in rocks or the earth will form acid mine drainage when exposed to oxidizing to metal mining, coal, and other large-scale excavations [1]. If there is high concentration of alkaline rich materials in the mine even in the presence of metal pyrite can still result to alkaline condition [2, 3]. The toxic wastewater produced from the mines is as a result of the oxidation of metal pyrite mine wastes/tailings with oxygen in the presence of water [4]. The AMD formed from the oxidation of pyritic metals is characterized with low pH, high electrical conductivity (EC), high total dissolved solids (TDS) and elevated sulphate concentration [5-9]. Acidity in AMD is composed of mineral acidity with the presence of iron, aluminum, manganese, and other metals depending on the soil geologic composition and metal sulphide and hydrogen ion acidity. Coal and Gold mines contains of more ferrous and ferric pyrite substances and rich in low concentration toxic metal ions [10-12]. AMD is a waste that is associated with mining and mineral processing activities all over the world especially where coal and gold mine activities are common [13-16]. AMD is one of the most prevalent causes of environmental pollution due to its high acidity ($pH < 3$) and toxic metal [16, 17]. Acid mine drainage (AMD) is a serious environmental issue which is associated with mining because of its acidic pH and potentially toxic elements (PTE) content. In chemical treatment of AMD, the conventional method of chemical treatments that are always used to treat AMD involves the addition of alkaline materials and other chemicals to neutralize it and enhance hydroxide precipitation [18]. All treatment methods have one shortcoming or the other due to one condition or the other [19, 20]. However, these chemical methods also generate large volumes of metal sludge which is another problem to the treatment process [21, 22]. Chemical reduction process involves the use of reducing agents such as sodium borohydride ($NaBH_4$), and hydrazine ($N_2H_2$) for metal recovery by chemical precipitation method [23]. Hydrazine is a powerful strong chemical reductant that is widely used in various chemical reactions for the synthesis of finely divided metals [24]. Different soluble metal ions are recovered as useful insoluble elemental zerovalent metal from chemical reduction instead of metal hydroxide sludge like chemical precipitation method [23]. As metal ions in the solution are immediately reduced to metallic state, the amount of metal ions in the solution is reduced. The metal reduction reaction proceeds according to the reaction presented in Equation (1) [23, 25]. The aim of this study is to use hydrazine to remove toxics heavy metals from AMD which eventually precipitated out metal ions in the solution and convert it to a zerovalent metal without generating sludge.

# 2. Materials and Methods

## 2.1. Sampling

The samples were collected from Navigation coal mine in Mpumalanga Province in the Republic of South Africa using plastic container and sealed immediately to prevent the ingress of air so as not to cause oxidation of the minerals in the mine water solution. The AMD sample was kept in a refrigerator at 4°C.

## 2.2. Chemical and Reagents

The chemicals used for this research were analytical grade reagents: hydrazine, concentrated nitric acid, hydrochloric acid, ethanol, reagent grade ferric sulphate salt and they were all purchased from Sigma Aldrich and Kimix chemical company. All chemicals were used without any further treatment.

## 2.3. Digestion

The AMD wastewater was digested using aqua regia consisting of $HNO_3$ and HCl in ratio 1: 3 after which it was quantified using ICP-OES instrument to determine the concentrations of the metal ions present in the AMD. The digestion of AMD was carried out to free the metals that are trapped in the matrix of the mineral ore.

## 2.4. Chemical Treatment

The chemical treatment of AMD was carried out using hydrazine by optimizing the concentration and contact time to obtain clean water. 50 mL of AMD sample was measured into a 250 mL conical flask and subjected to constant stirring titrated with 100 mL 1 M $N_2H_2$ reagent and the mixture was stirred constantly of a hotplate magnetic stirrer regulated at 60°C for 2 hours. Addition of hydrazine into the mixture at 60°C and brown precipitate was formed and continue the addition until there was no brown particle formed [26]. Filter the mixture and collect the residue and the supernatant solution for ICP-OES quantification while the residue was washed with distilled water several times before it subjected to drying with nitrogen gas or freeze dryer. The dried residue was kept in a sample bottle until it is required for characterization using XRD, XRF, FTIR and SEM analysis. Contact time conducted at 5, 15, 30, 45, 60 and 120 minutes to obtain clean water using optimized concentration of hydrazine. 50 mL of AMD sample was measured into different 250 mL conical flask and stirred constantly of a hotplate magnetic stirrer regulated at 60°C for 2 hours, add 100 mL 0.6 M $N_2H_2$ reagent into the mixture to form brown precipitate, continue the addition until the brown particle stopped to form. Filter the mixture, collect the supernatant solution for ICP-OES quantification while the residue was washed with distilled water several times before it subjected to drying with nitrogen gas or freeze dryer. The dried residue was grinded, sieve and kept in a sample bottle until it is required for characterization using XRD, XRF, FTIR SEM, and TEM analysis.

Equation of Reaction

$$M^{m+}(aq) + N_2H_4(l) \rightarrow M^0(s) + N_2(g) + H^+(aq) \quad (1)$$

$$Fe^{3+} + N_2H_4 \rightarrow Fe^0(s) + N_2(g) + 4\,H^+(aq) \quad (2)$$

$$Fe^0(s) + H_2O(l) + O_2(g) \rightarrow FeOOH \quad (3)$$

### 2.4.1. Concentration Optimization

The concentration of hydrazine solution used in the chemical treatment of AMD was optimized using 0.1, 0.2, 0.3, 0.4, 0.5, 0.6, 0.7, 0.8, 0.9, and 1.0 M.

### 2.4.2. Contact Time Optimization

The contact time of the hydrazine chemical treatment of AMD was optimized using the contact time of 5, 15, 30, 45, 60 and 120 minutes.

The percentage removal of metal (% R) was calculated using the equation,

$$\%\ R = C_0\text{-}C_e/C_0 \times 100\% \quad (4)$$

## 2.5. Characterization

The chemical composition of the AMD cations and anions were determined with Varian Radial Inductively Coupled Plasma Optical Emission Spectroscopy (ICP-OES) and Dionex DX-120 Ion Chromatography respectively. The crystallinity, particle size and mineral phases of the brown residue was identified with an x-ray powder diffraction patterns were obtained using on a Bruker D8 Advance x-ray diffractometer with Cu Kα radiation (45kV, 40mA, λ = 1.542Å), scanned from 20 to 80 ° (2θ). The morphology and particle size of the residue was examined with a scanning electron microscopy (SEM EDS) which was conducted using a HITACHI S-4700 electron microscope. The HRTEM morphological analysis was carried out on the precipitate using Phillips Tecnai F20 super-twain TEM. XRF elemental composition of precipitate was carried out using a Philips PW 2400 X-ray sequential spectrophotometer to determine the elemental constituents of the precipitated sample. The FTIR was used to determine the functional groups present in the rice husk samples using attenuated total reflectance (ATR). The FTIR spectroscopy was used to determine functional groups present in the precipitate with attenuated total reflectance (ATR). The particle was dried in an oven regulated at 105°C for 24 hours to remove any trace of moisture present in the precipitated particles.

# 3. Results

## 3.1. Physicochemical Parameters

The physicochemical analysis of the AMD conducted are pH, electrical conductivity (EC), total dissolved solids (TDS), temperature, dissolved oxygen (DO) is presented in Figure 1. The results of the physicochemical parameters are not within the WHO permissible limit of drinking water and it implies the discharge into natural water body will lead to serious water pollution [27].

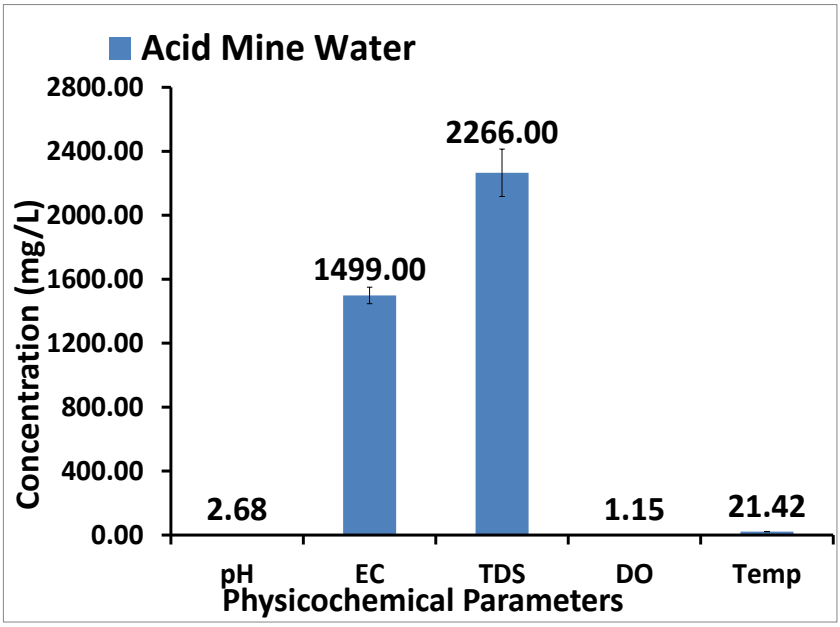


*Figure 1. Physicochemical analysis of AMD wastewater.*

*Table 1. Physicochemical Analysis of AMD.*

| Physicochemical Parameters | WHO Standard |
|---|---|
| pH | 6.5-8.5 |
| EC | ≤ 400 µScm |
| TDS | 300–600 mg/L |
| DO | |
| Temperature | ≤ 25°C |

## 3.2. Cations and Anions Analysis

The cation and anion analysis of the AMD was using ICP-OES and IC to determine the concentration of all the dissolved ions in solution are presented in Figures 2 and 3. Figures 2 and 3 present the concentrations of all the dissolved metals and anions in the RAMD solution respectively. The ICP concentration (4492.13 mg/L) results indicated 70.42% iron content as the predominant cation while the IC concentration (27,731.81 mg/L) results indicated 99.73% sulphate content. The cation and anion analysis revealed that AMD sample was rich in iron and sulphate ions which mean that the sample can be used as feedstock raw material substitute of reagent grade iron salt for making iron nanoparticles. The ICP-OES and IC results are presented in Figures 1 and 2 respectively.

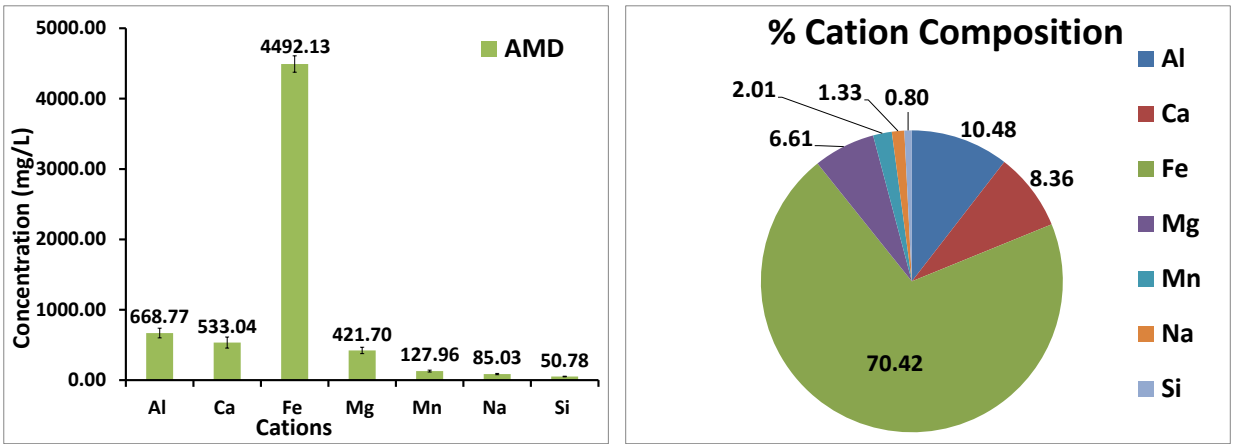


*Figure 2. Cation Concentration (A) and% Cation Composition (B) in Acid mine wastewater.*

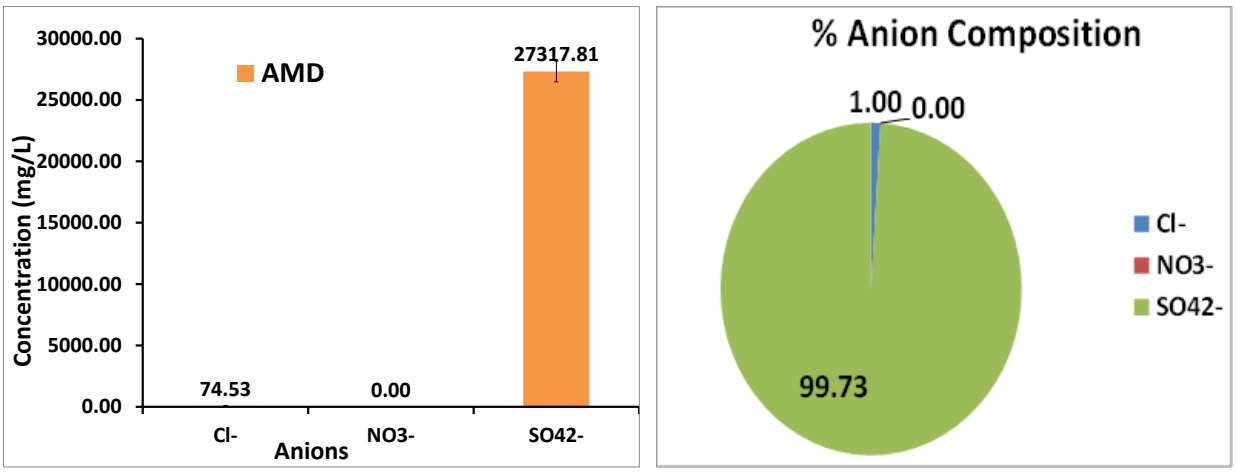


*Figure 3. Anion Concentration and% Anion Composition in Acid mine wastewater.*

## 3.3. Hydrazine Chemical Treatment Optimization

The removal of toxic heavy metals by chemical treatment of the AMD was carried out using hydrazine ($N_2H_2$) by optimizing the concentration of hydrazine solution using 0.1, 0.2, 0.3, 0.4, 0.5, 0.6, 0.7, 0.8, 0.9, and 1.0 M and contact time using 20, 40, 60, 80, 100 and 120 minutes.

### 3.3.1. Concentration Optimization

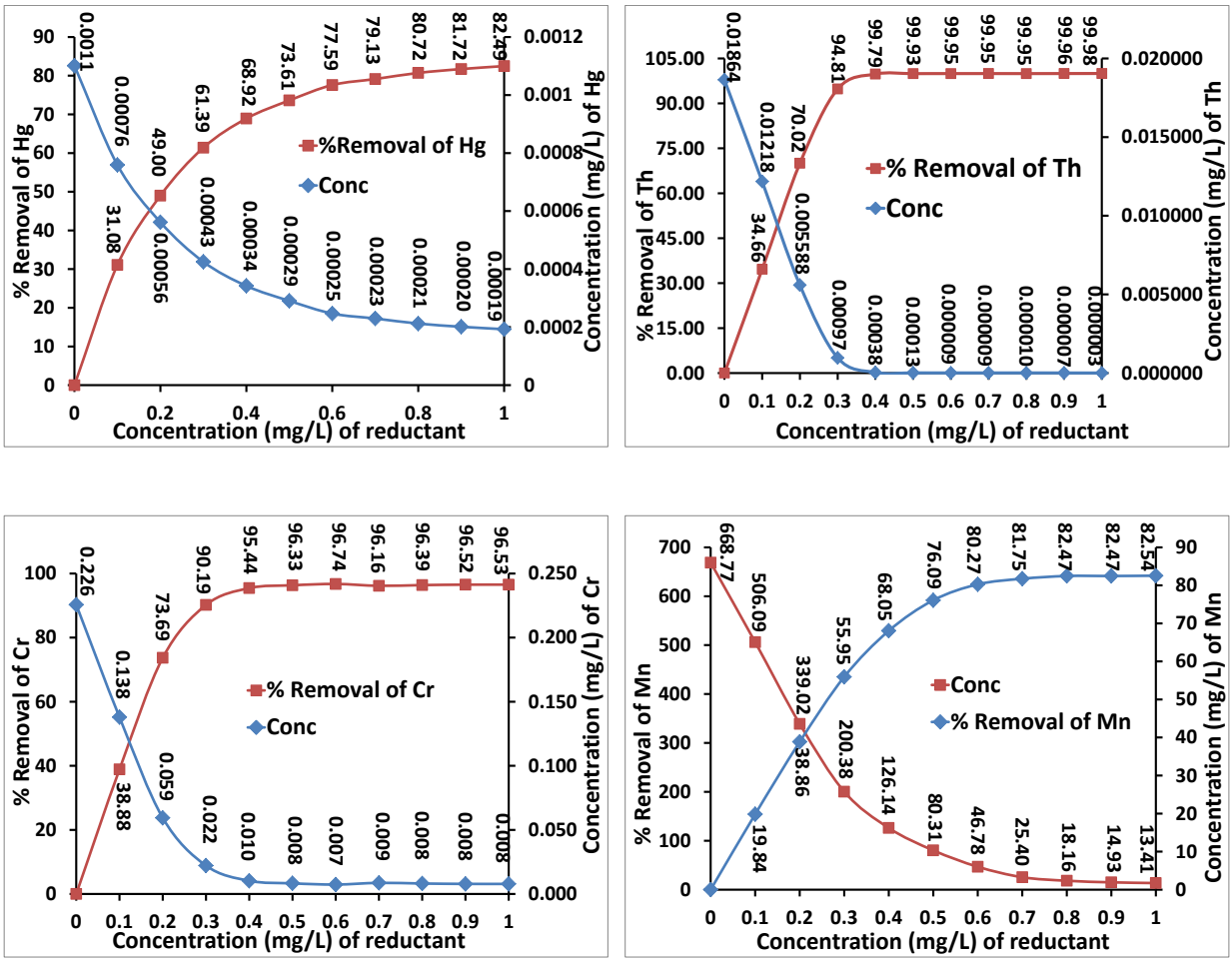


*Figure 3. Concentration Effect of Hydrazine removal of Hg, Th, Cr and Mn in AMD.*

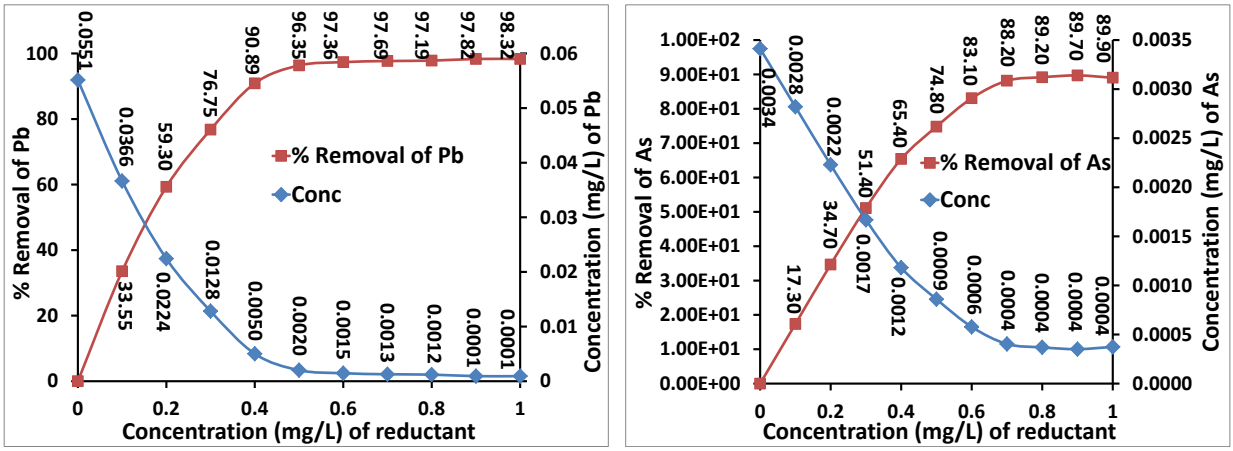

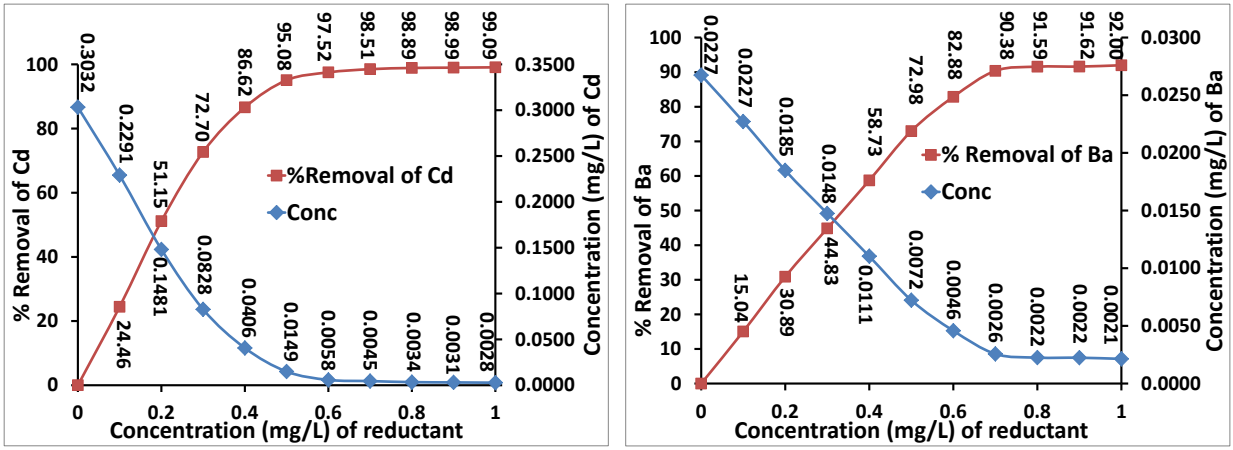


***Figure 4.*** *Concentration Effect of Hydrazine removal of Pb, As, Cd and Ba in AMD.*

The concentration of hydrazine treatment removal of toxic heavy metals in acid mine drainage wastewater was optimized using 0.1, 0.2, 0.3, 0.4, 0.5, 0.6, 0.7, 0.8, 0.9, and 1.0 M is presented in Figures 3-4. The hydrazine treatment removal of Hg, Th, Cr and Mn were optimized using 0.1–1.0 M $N_2H_2$ solution is presented in Figure 3 and the $N_2H_2$ treatment removal of Pb, As, Cd and Ba is presented in Figure 4. Figure 3 presents the concentration of Hg reduced from 0.0011 M to 0.00019 M to obtain a maximum removal of 82.49%, Th reduced from 0.01864 M to 0.000003 M with a maximum removal of 99.98%, Cr 0.226 M to 0.008 M with maximum removal of 96.53%, and Mn 668.77 M to 13.41 M with maximum removal of 82.54%. Figure 4 presents the concentration of Pb 0.0551 M reduced to 0.0001 M with maximum removal of 98.32%, As 0.0034 M to 0.0004 M with maximum removal of 89.90%, Cd 0.3032 M reduced to 0.0028 M with a maximum removal of 99.09% and Ba 0.00227 M to 0.0021 M with a removal of 92.00%. As the concentration of hydrazine increase, the concentration of the toxic heavy metals in the AMD decrease and the percent removal of toxic heavy metals increase.

### 3.3.2. Contact Time Optimization

The removal of toxic heavy metals in AMD using hydrazine chemical for treatment was optimized at contact time of 5, 15, 30, 45, 60, and 120 minutes. The contact time of hydrazine treatment removal of toxic heavy metals in AMD was optimized at 5, 15, 30, 45, 60, and 120 minutes is presented in Figures 5-6. The contact time hydrazine treatment removal of Hg, Th, Cr and Mn in the AMD was optimized at 20-120 minutes is presented in Figure 5. The contact time hydrazine treatment of Pb, As, Cd and Ba Figure 5 presents the contact time of Hg reduced from 0.0011 M to 0.00025 M to obtain a maximum removal of 77.59%, Th 0.055 M reduced to 0.004 M with a maximum removal of 91.85%, Cr 0.063 M to 0.008 M with maximum removal of 87.10%, and Mn 127.78 M to 4.33 M with maximum removal of 96.61%. Figure 6 presents the conc of Pb 0.0034 M reduced to 0.0002 M with maximum removal of 82.32%, As 0.055 M to 0.010 M with maximum removal of 82.32%, Cd 0.3032 M reduced to 0.006 M with a maximum removal of 93.04% and Ba 0.00227 M to 0.00010 M with a removal of 96.010%. As the contact time of the treatment increase, the concentration of the AMD toxic heavy metals decrease and the percent removal of toxic heavy metals increase.

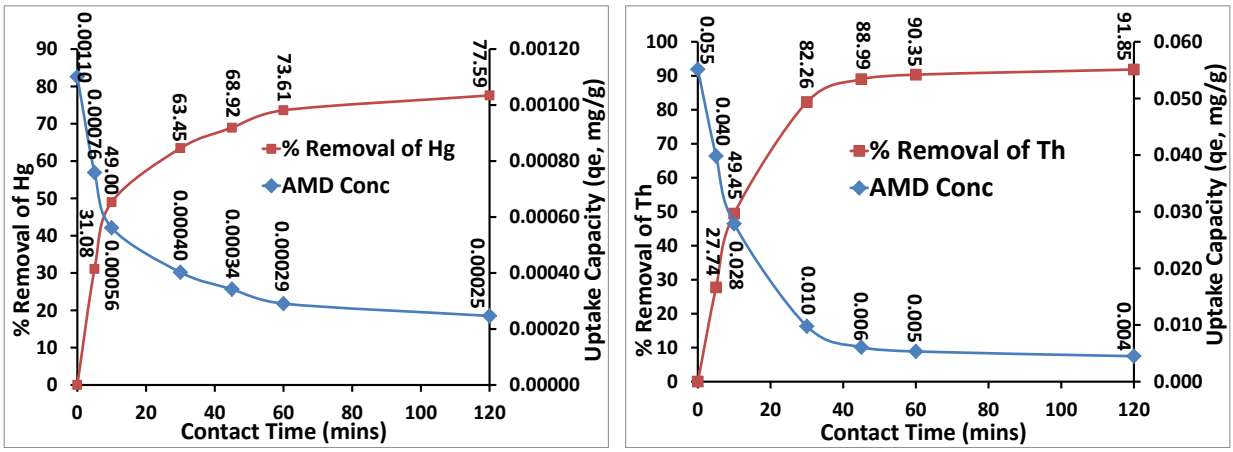

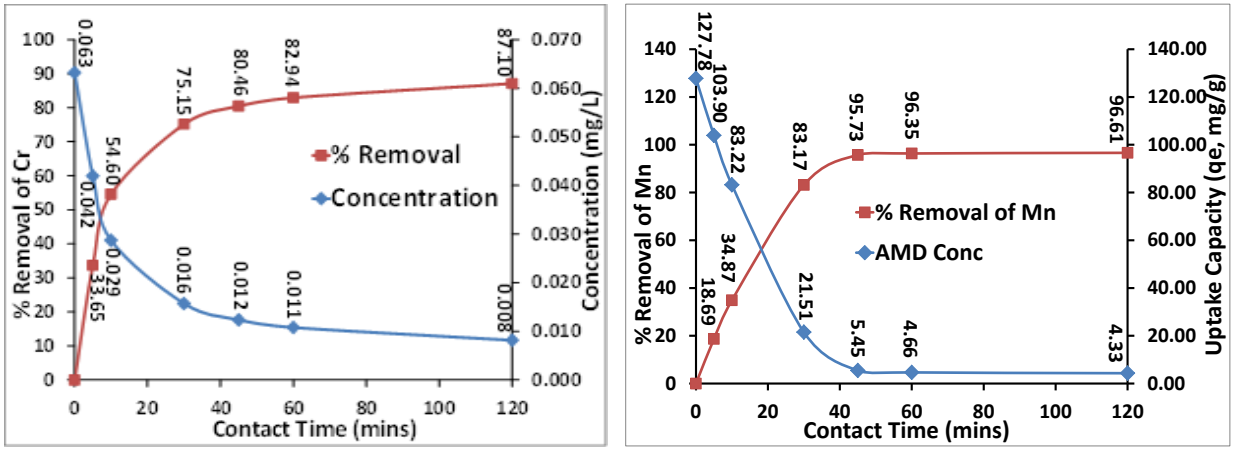


*Figure 5. Contact Time Effect of Hydrazine removal of Hg, Th, Cr and Mn in AMD.*

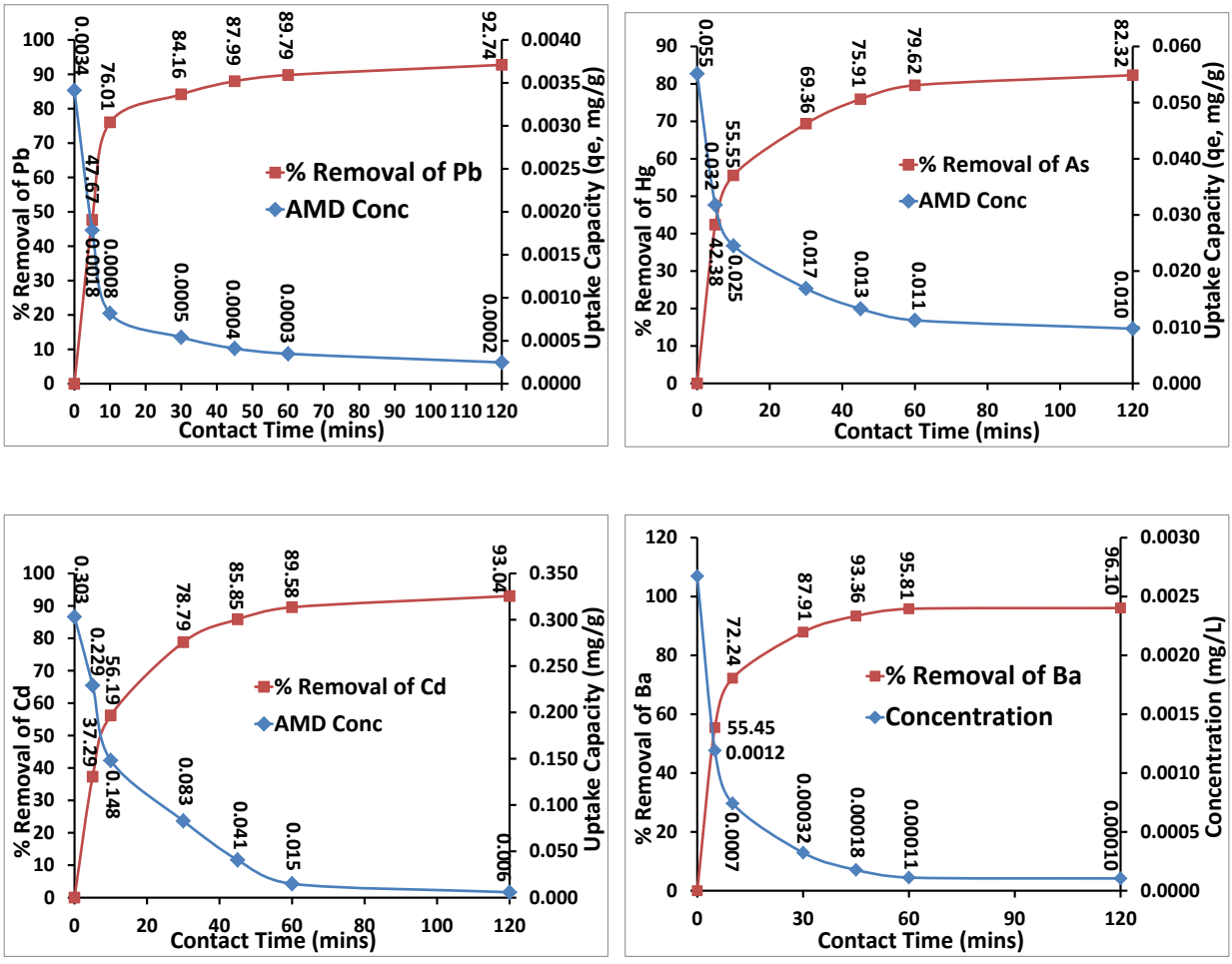


*Figure 6. Contact Time Effect of Hydrazine removal of Pb, As, Cd and Ba in AMD.*

## 3.4. Characterization

### 3.4.1. XRD and XRF

Figure 7 presents the XRD spectrum and XRF elemental composition of hydrazine precipitated Fe from iron rich AMD. The XRD spectrun using JCPDS database at reflection angles revealed where characteristic peaks of a particular mineral phase can be seen on the spectrum. The diffraction pattern of peaks exhibited by the precipitated Fe whose reflection angles are indexed at 21.88°, 26.46°, 33.85°, 47.79°, 54.2°, 63.38°, 65.84°, 71.12° and 79.12° corresponds to goethite mineral phase. This diffraction pattern of the precipitated Fe can be indexed to goethite [α-FeO(OH)] mineral phase and the peaks agrees with previously reported literature Jaiswal et al., [28];

Taleb et al., [29]; Flores et al., [30] and the peaks are tiny which shows that the particles have smaller crystal size and crystalline [31]. The diffraction peak at reflection angle indexed at 45.5° corresponded to pure iron (α-Fe) mineral phase which indicate the presence of zerovalent iron (α-Fe) with some traces of amorphous crystallinity [28, 32]. All available reflections of the present XRD peaks can be attributed to the presence of goethite The sharp and strong diffraction reflection peaks, revealed the residue to be crystalline nanoparticles. The XRF elemental composition of the precipitated Fe from hydrazine treated AMD is presented in Figure 7. The results revealed the chemical composition of the precipitated Fe sample was composed of majorly iron (Fe) particles of about 96.9 ± 0.36%. The other elements precipitated elemental composition are trace amount such as Al (1.19%), Si (0.4%), Ca (0.28%) and Mg (0.46%) can be attributed to the source of the iron salt solution. Previous study revealed that the XRF results usually showed that Fe have the highest composition in any goethite mineral sample [33, 34].

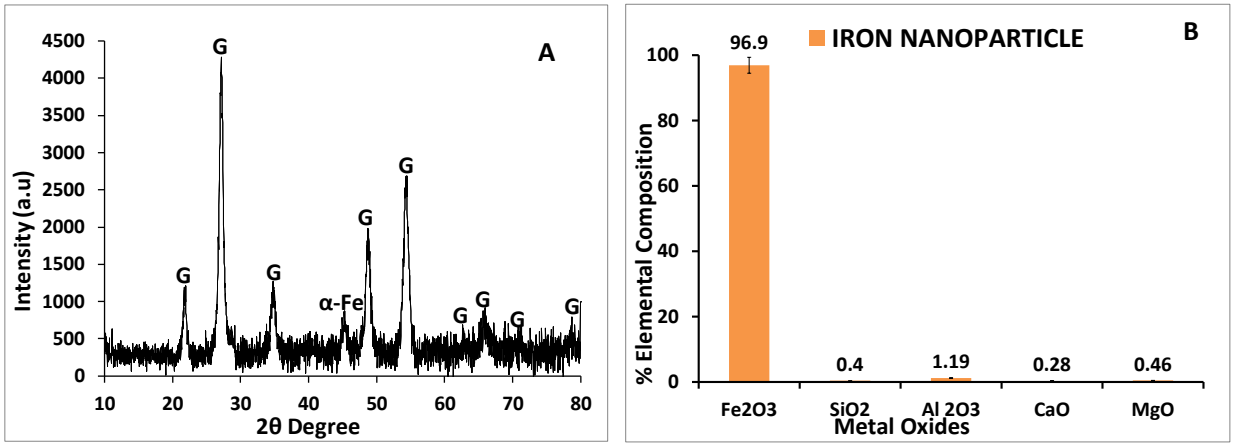


***Figure 7.*** *XRD spectrum analysis (A) and XRF elemental composition (B) of HTAR precipitate.*

### 3.4.2. SEM and TEM

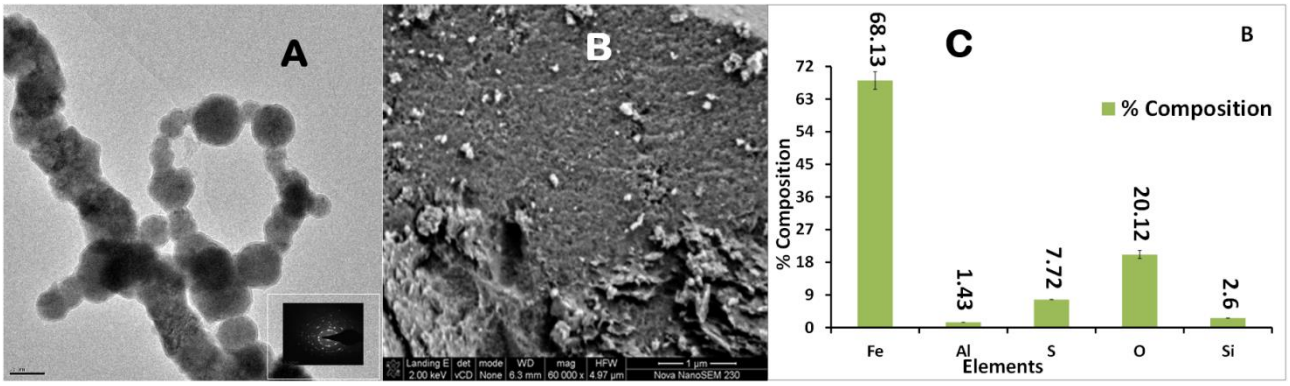


***Figure 8.*** *TEM-SAED (A), SEM image (B) o and SEM-EDS elemental composition (C) of HTAR precipitate.*

Figure 8 presents the SEM and TEM morphology of the precipitates obtained from the chemical reduction treatment of AMD using hydrazine reagent. The TEM micrograph analysis of the precipitated Fe from AMD is presented in Figure 8A which shows that the particles are spherical in shape with particle sizes determined using ImageJ software to be 6.78 ± 1.12 nm. The ring-type pattern of the selected area electron diffraction (SAED) analysis of the precipitated Fe revealed that the particle was crystalline and monodispersed with the ring. The morphology of the precipitate Fe revealed a spherical bead-like shape with SAED indicating crystallinity [35]. Previous studies revealed that hydrazine precipitated Fe are spherical with particles sizes to be higher than and less than 7 nm and 5 nm [36]. The SEM is a technique used to determine the shape, texture and surface morphology of a sample and the shape of precipitated Fe from the iron-rich AMD was spherical in shape with some long tiny strands [6, 37]. The SEM-EDS of the chemically precipitated residues in Figure 8B & C revealed

the particle sizes ranging from 48-64 nm. The EDS gives accurate information of the type of elements present in the precipitated sample but not the accurate quantities of the elements are Fe (68.13%), Al (1.43%), S (7.72%), O (20.12%) and Si (2.6%) and it implies that Fe constitute bulk of the particles precipitated from the chemical reduction process. The EDS elemental analysis revealed that the precipitated Fe contained very high percentage of Fe (68.13%) for the metals and non metals [S (7.72%) and O (30.12%)] identified with the ICP-OES and IC results in Figure 2 to confirm Fe and sulphate were the predominant cation and anion respectively. The SEM-EDS result confirm the XRF elemental composition of the precipitated Fe.

### 3.4.3. FTIR

The FTIR absorption spectra of precipitated residue from chemical treated AMD is presented in Figure 4. FT-IR spectra of the precipitated goethite mineral revealed a very broad band of O–H at 3262.48 $cm^{-1}$ which can be attributed to the stretching vibration of $H_2O$ molecules. Strong C=O absorption stretching bands at 2525.82 $cm^{-1}$–2037.71 $cm^{-1}$ can be assigned to the presence of $CO_3^{-2}$ due to contamination by atmospheric $CO_2$ and it revealed that residue Fe has strong affinity for $CO_2$ gas [28, 31, 38]. The sharp peak at 1668.39 $cm^{-1}$ can be ascribed to the O–H bending of water molecules [28, 39-41]. The IR absorption band at 1096.14 $cm^{-1}$ can be attributed to the presence of S–O bond. The characteristic sharp bands at 817.32 $cm^{-1}$ and 700.36 $cm^{-1}$ can be assigned to the Fe–O–OH bending vibration in a-FeOOH [38, 42, 43]. The weak IR stretching bands between 1096.14 $cm^{-1}$ and 993.09 $cm^{-1}$ can be due to the presence of a trace amount of quartz [42]. These IR bands of 873.27 $cm^{-1}$ and 700.32 $cm^{-1}$ were assigned to Fe–O–H in-plane bending (δOH) and out-of-plane bending (γOH) vibrations respectively The 612.17 $cm^{-1}$ band is ascribed to Fe–O stretching vibrations of goethite [28, 44].

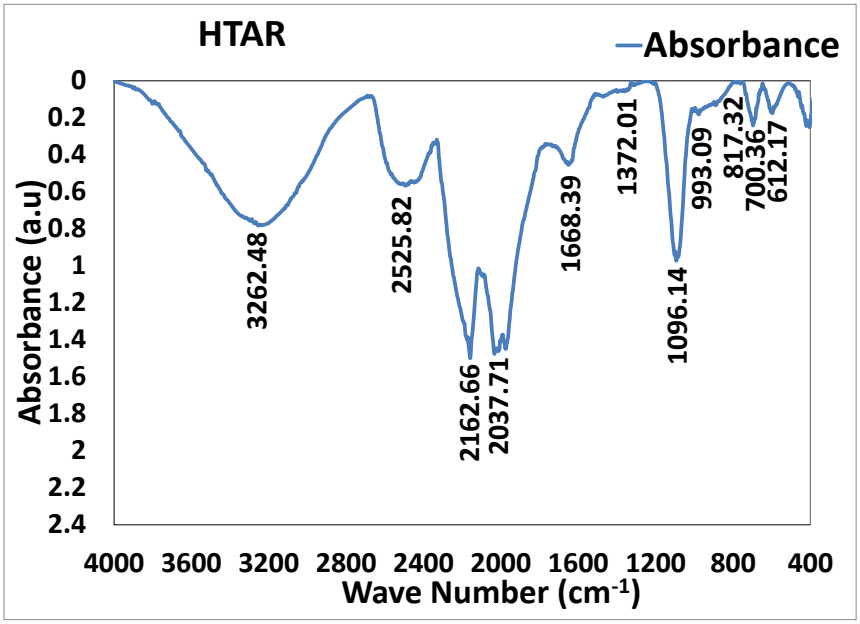


***Figure 9.*** *FTIR absorption bands of HTAR precipitate.*

## 4. Conclusion

1) This study revealed that in the course of treating the iron rich AMD with hydrazine chemical reductant, the played dual role of reducing the Fe in the AMD to Fe precipitate and the same time cleaning the water by removing colour and toxic heavy metals.
2) The concentrations of the toxic metals from the AMD wastewater were removed by the hydrazine chemical at very high percentage and also making the concentrations to fall within the WHO permissible standard limit.
3) The physicochemical analysis showed that AMD wastewater was contaminated and some parameters were within the WHO drinking water permissible limit.
4) Analysis of the raw AMD wastewater for cations and anions revealed that it contained Fe and $SO_4$ as the predominant cation and anion.
5) Chemical reduction treatment of the AMD using hydrazine chemical generated less volume of waste which was a valuable nanomaterial and can be used for environmental cleaning of wastewater.
6) Characterization of the residue generated from the hydrazine chemical treatment using XRD, XRF, SEM EDS, TEM and FTIR the results are: XRD identified goethite mineral phase, crystallinity and particles size of 7.43 nm; XRF elemental composition revealed 96.8% Fe in the

precipitate, 12% $Al_2O_3$, 0.34% $SiO_2$, 0.25% CaO and 1.32% MgO; TEM showed crystallinity, and particle size of 8.9 nm; SEM revealed the surface morphology which was spherical with particle size of 56 97 nm and FTIR revealed the functional groups in the residue which identified O–H, C–H, C=O, Fe–O–O–H, S–O, Fe–O–O–H, Fe–O stretching and C–H bending.

7) Chemical reductants are good reagent for treatment of AMD by precipitating impurities to generate low volume of waste, with a valuable product that can be used for other purposes.
8) The chemical treatment yielded high percentage removal of some toxic heavy metals from the AMD.

## Abbreviations

| | |
|---|---|
| AMD | Acid Mine Drainage |
| IC | Ion Chromatography |
| ICP-OES | Inductively Coupled Plasma-Optical Emission Spectroscopy |
| HTAR | Hydrazine Treated AMD Residue |
| XRD | X-ray Diffraction |
| XRF | X-ray Flourescence |
| SEM-EDS | Scanning Electron Microscopy-Energy Dispersive Spectroscopy |
| TEM | Transmission Electron Microscopy |
| SAED | Selected Area Electron Dispersion |
| FTIR | Fourier Transform Infrared Spectroscopy |
| IR | Infrared |
| $N_2H_2$ | Hydrazine |

## Acknowledgments

The authors wish to acknowledge Mrs. Omowonuola, A. A for the technical assistance and Lagos State University management for giving us the enabling environment for conducting the research.

## Author Contributions

**Alegbe Mondat John:** Conceptualization, Methodology, Resources
**Moronkola Bridget Adekemi:** Data Curation
**Fatoba Oolanrewaju Ojo:** Formal Analysis
**Adekolurejo Ezekiel:** Investigation
**Agboola Olugbenga Ayodeji:** Project Administration
**Oyesomi Aisha:** Project Administration
**Petrik Leslie Felicia:** Funding Acquisition

## Conflicts of Interest

The authors have no conflicts of interest.

## References

[1] Skousen, J., Rose, A., Geidel, G., Foreman, J., Evans, R., & Hellier, W. (1999). Handbook of technologies for avoidance and remediation of acid mine drainage. National Mine Land Reclamation Center, West Virginia University, Morgantown, WV. https://www.osmre.gov/resources/library/ghm/hbtechavoid.pdf

[2] Skousen, J., Simmons, J., McDonald, L., & Ziemkiewicz, P. 2002. Acid-base accounting to predict post-mining drainage quality on surface mines. *J. Environ. Qual*. 31: 2034-2044. https://doi.org/10.2134/jeq2002.2034

[3] Skousen, J. (2014). Overview of acid mine drainage treatment with chemicals. Acid mine drainage, rock drainage, and acid sulfate soils: Causes, assessment, prediction, prevention, and remediation, 325-337.

[4] Retka, J., Rzepa, G., Bajda, T., & Drewniak, L. (2020). The use of mining waste materials for the treatment of acid and alkaline mine wastewater. *Minerals*, 10(12), 1061.

[5] Alegbe, M. J., Ayanda, O. S., Ndungu, P., Nechaev, A., Fatoba, O. O., & Petrik, L. F. (2019). Physicochemical characteristics of acid mine drainage, simultaneous remediation and use as feedstock for value added products. *Journal of Environmental Chemical Engineering*, 7(3), 103097.

[6] Alegbe, M. J., Moronkola, B. A., Osundiya, M. O., Adekolurejo, E., Ajewole, B. S., & Petrik, L. F. (2022). Synthesis of iron nanoparticles from acid mine drainage using hydrazine as reductant. *Am. J. Chem*, 12, 23-31.

[7] Hatar, H., Rahim, S. A., Razi, W. M., & Sahrani, F. K. (2013, November). Heavy metals content in acid mine drainage at abandoned and active mining area. In AIP conference proceedings (Vol. 1571, No. 1, pp. 641-646). *American Institute of Physics*.

[8] McCarthy, T. S. (2011). The impact of acid mine drainage in South Africa. *South African Journal of Science,* 107(5), 1-7.

[9] Cheng, H., Hu, Y., Luo, J., Xu, B., & Zhao, J. (2009). Geochemical processes controlling fate and transport of arsenic in acid mine drainage (AMD) and natural systems. *Journal of hazardous materials*, 165(1-3), 13-26.

[10] Menshikova, E., Osovetsky, B., Blinov, S., & Belkin, P. (2020). Mineral formation under the influence of mine waters (the Kizel Coal Basin, Russia). *Minerals*, 10(4), 364.

[11] Sahoo, P. K., Tripathy, S., Panigrahi, M. K., & Equeenuddin, S. M. (2014). Geochemical characterization of coal and waste rocks from a high sulfur bearing coalfield, India: Implication for acid and metal generation. *Journal of geochemical Exploration*, 145, 135-147.

[12] Aghaei, E., Wang, Z., Tadesse, B., Tabelin, C. B., Quadir, Z., & Alorro, R. D. (2021). Performance evaluation of Fe-Al bimetallic particles for the removal of potentially toxic elements from combined acid mine drainage-effluents from refractory gold ore processing. *Minerals*, 11(6), 590, 2021.

[13] Ojonimi, T. I., Chanda, T. P., & Ameh, E. G. (2021). Acid mine drainage (AMD) contamination in coal mines and the need for extensive prediction and remediation: a review. *Journal of Degraded and Mining Lands Management*, 9(1), 3129-3136.

[14] Kefeni, K. K., Msagati, T. A., & Mamba, B. B. (2017). Acid mine drainage: Prevention, treatment options, and resource recovery: A review. *Journal of cleaner production*, 151, 475-493, 2017.

[15] Kefeni, K. K., Msagati, T. A., Nkambule, T. T., & Mamba, B. B. (2018). Synthesis and application of hematite nanoparticles for acid mine drainage treatment. *Journal of Environmental Chemical Engineering*, 6(2), 1865-1874.

[16] Naidu, G., Ryu, S., Thiruvenkatachari, R., Choi, Y., Jeong, S., & Vigneswaran, S. (2019). A critical review on remediation, reuse, and resource recovery from acid mine drainage. *Environmental pollution*, 247, 1110-1124.

[17] Naidu, T. S., Sheridan, C. M., & Van Dyk, L. D. (2021). Design of Acid Mine Drainage Remediation Plant.

[18] Masindi, V., Akinwekomi, V., Maree, J. P., & Muedi, K. L. (2017). Comparison of mine water neutralisation efficiencies of different alkaline generating agents. *Journal of environmental chemical engineering*, 5(4), 3903-3913.

[19] Trumm, D. 2010. Selection of active and passive treatment systems for AMD-flow charts for New Zealand conditions. *New Zealand J. of Geology and Geophysics* 53: 195-210. https://doi.org/10.1080/00288306.2010.500715

[20] Kalin, M., Fyson, A., & Wheeler, W. N. (2006). The chemistry of conventional and alternative treatment systems for the neutralization of acid mine drainage. *Science of the total environment*, 366(2-3), 395-408.

[21] Kim, Y. S., Kim, D. H., Yang, J. S., & Baek, K., (2012). Adsorption characteristics of As (III) and As (V) on alum sludge from water purification facilities. Sep. *Sci. Technol*. 47(14–15), 2211–2217.

[22] Sithole, N. T., & Ntuli, F. (2022). Evaluation of hydrazine, dimethylamine borane and glyoxylic acid as reducing agents in reductive precipitation. *South African Journal of Chemical Engineering*, 41, 17-25.

[23] Chen, J. P., & Lim, L. L. (2002). Key factors in chemical reduction by hydrazine for recovery of precious metals. Chemosphere, 49(4), 363-370.

[24] Mashifan, T., & Sithole, N. (2019). Reduction crystallization of heavy metals from acid treated phosphogypsum effluent utilizing hydrazine as a reducing reagent. In E3S Web of Conferences (Vol. 96, p. 01002). EDP Sciences.

[25] Fanning, J. C., Brooks, B. C., Hoeglund, A. B., Pelletier, D. A., & Wadford, J. A. (2000). The reduction of nitrate and nitrite ions in basic solution with sodium borohydride in the presence of copper (II) ions. Inorganica Chimica Acta, 310(1), 115-119.

[26] Manuel, J. R., & Clout, J. M. F. (2017). Goethite classification, distribution and properties with reference to Australian iron deposits. *Proc. Iron Ore*, 567-574.

[27] WHO, Guidelines for drinking-water quality – 4th ed. World Health Organization, 2011.

[28] Jaiswal, A., Banerjee, S., Mani, R., & Chattopadhyaya, M. C. (2013). Synthesis, characterization and application of goethite mineral as an adsorbent. Journal of Environmental Chemical Engineering, 1(3), 281-289.

[29] Taleb, K., Markovski, J., Hristovski, K. D., Rajaković-Ognjanović, V. N., Onjia, A., & Marinković, A. (2016). Aminated glycidyl methacrylates as a support media for goethite nanoparticle enabled hybrid sorbents for arsenic removal: From copolymer synthesis to full-scale system modeling. *Resource-Efficient Technologies*, *2*(1), 15-22.

[30] Flores, R. G., Andersen, S. L. F., Maia, L. K. K., José, H. J., & Moreira, R. d. F. P. M. (2012). Recovery of iron oxides from acid mine drainage and their application as adsorbent or catalyst. *Journal of Environmental Management*, 111, 53-60.

[31] Ghosh Chaudhuri, R., & Paria, S. (2012). Core/shell nanoparticles: classes, properties, synthesis mechanisms, characterization, and applications. Chemical reviews, 112(4), 2373-2433.

[32] Yuvakkumar, R., Elango, V., Rajendran, V., & Kannan, N. (2011). Preparation and characterization of zero valent iron nanoparticles. Digest Journal of Nanomaterials and Biostructures, 6(4, October-December), 1771-1776, 2011.

[33] Shaltout, A. A., Gomma, M. M., & Ali-Bik, M. W. (2012). Utilization of standardless analysis algorithms using WDXRF and XRD for Egyptian iron ore identification. *X-Ray Spectrometry*, *41*(6), 355-362.

[34] Donskoi, E., Manuel, J. R., Hapugoda, S., Poliakov, A., Raynlyn, T., Austin, P., & Peterson, M. (2022). Automated optical image analysis of goethitic iron ores. *Mineral Processing and Extractive Metallurgy*, *131*(1), 14-24.

[35] Lassoued, A., Dkhil, B., Gadri, A., & Ammar, S. (2017). Control of the shape and size of iron oxide ($\alpha$-$Fe_2O_3$) nanoparticles synthesized through the chemical precipitation method. *Results in physics*, *7*, 3007-3015.

[36] Mohapatra, M., & Anand, S. (2010). Synthesis and applications of nano-structured iron oxides/hydroxides–a review. *International Journal of Engineering, Science and Technology*, *2*(8).

[37] Abdus-Salam, N., & Itiola, A. D. (2012). Potential application of termite mound for adsorption and removal of Pb (II) from aqueous solutions. *Journal of the Iranian Chemical Society*, *9*(3), 373-382.

[38] Salami, N & Adekola, F. A, (2002). A study of sorption of cadmium by goethite in aqueous solution, *Bull. Chem. Soc. Ethiop*. 16(2002) 1–7.

[39] Li, M., Liu, H., Chen, T., Hayat, T., Alharbi, N. S., & Chen, C. (2017). Adsorption of Europium on Al-substituted goethite. *Journal of Molecular Liquids*, *236*, 445-451.

[40] Gotic, M, Music S, Popovic S, Sekovanic, L (2008). Investigation of factors influencing the precipitation of iron oxides from Fe(II) containing solutions, Croat. Chem. Acta 81(2008) 569–578.

[41] Duhan, S., & Devi, S. (2010). Synthesis and structural characterization of iron oxide-silica nanocomposites prepared by the sol gel method. *International Journal of Electronics Engineering*, *2*(1), 89-92.

[42] Ristić, M., Opačak, I., & Musić, S. (2013). The synthesis and microstructure of goethite particles precipitated in highly alkaline media. Journal of alloys and compounds, 559, 49-56.

[43] Ramirez-Muniz, K., Perez-Rodriguez, F., & Rangel-Mendez, R. (2018). Adsorption of arsenic onto an environmentally friendly goethite-polyacrylamide composite. *Journal of Molecular Liquids*, *264*, 253-260.

[44] Parida, K., & Das, J. (1996). Studies on ferric oxide hydroxides: II. Structural properties of goethite samples (α-FeOOH) prepared by homogeneous precipitation from $Fe(NO_3)_3$ solution in the presence of sulfate ions. *Journal of colloid and interface science*, *178*(2), 586-593.